E11-2024-17

I. S. Gordeev [1,2,*], A. N. Bugay [1,2]

COMPUTER MODELING OF A NEW TYPE GALACTIC COSMIC RAYS SIMULATOR

Submitted to “Computer Physics Communications”

[1] Joint Institute for Nuclear Research, Dubna
[2] Dubna State University, Dubna, Russia
[*] E-mail: gordeev@jinr.ru

Гордеев И. С., Бугай А. Н. E11-2024-17

Компьютерное моделирование симулятора галактических космических лучей нового типа

Предлагаемый в Лаборатории радиационной биологии ОИЯИ симулятор галактических космических лучей (ГКЛ) нового типа потенциально способен создавать на ускорителях заряженных частиц смешанное поле излучения с включением множества ионов с широким диапазоном значений энергии и с необходимой распространенностью. Данное сложное многокомпонентное радиационное поле является имитацией радиационных условий, создающихся внутри корабля в космосе, при межпланетном перелете, например, на Марс. Приводится аналитическое описание симулятора ГКЛ, а также описание специально разработанного программного обеспечения, при помощи которого возможно подобрать необходимые параметры модели симулятора для создания интересующих радиационных условий смешанного излучения. В программном обеспечении реализована обработка данных, полученных на основе Монте-Карло программ FLUKA и PHITS, подбор и оптимизация параметров модели, а также средства визуализации данных.

Работа выполнена в Лаборатории радиационной биологии ОИЯИ.

Препринт Объединенного института ядерных исследований. Дубна, 2024

Gordeev I. S., Bugay A. N. E11-2024-17

Computer Modeling of a New Type Galactic Cosmic Rays Simulator

A new type of a galactic cosmic rays (GCR) simulator, provided at the JINR Laboratory of Radiation Biology, is potentially capable of generating a complex radiation field with inclusions of a variety of ions with a wide energy range and with required abundance at the charged particle accelerators. This complex multicomponent radiation field simulates radiation environment inside a spacecraft during an interplanetary flight, for example, to Mars. The paper provides an analytical description of the GCR simulator as well as a description of a specially developed software that enables selection of necessary parameters of a simulator model for creating relevant mixed radiation conditions. The software implements processing of data obtained with Monte Carlo-based FLUKA and PHITS programs, fitting and optimization of model parameters as well as data visualization tools.

The investigation has been performed at the Laboratory of Radiation Biology, JINR.

Preprint of the Joint Institute for Nuclear Research. Dubna, 2024

INTRODUCTION

Radiation is one of the major limiting factors of space exploration [1–3]. Cosmic radiation is represented by a wide diversity of particle types as well as their energies. Galactic cosmic rays (GCR) potentially pose maximum danger to the astronauts during interplanetary flights due to the complex radiation being constantly present in space while propagating isotropically. The main components of GCR are nuclei of elements with Z ranging between 1 and 28. In terms of flux, 99% are protons and helium nuclei, while the remaining 1% is high-energy charged particles (HZE ions) [4]. Despite the latter constituting a relatively small part in the GCR composition, they potentially pose a greater danger to the astronauts performing interplanetary flights owing to the high biological effectiveness of HZE ions. Such a complex and joint action of all the particles that compose GCR should be carefully studied in terrestrial conditions prior to carrying out interplanetary flights.

Modern charged particle accelerators essentially present the only instrument that makes it possible to recreate the effect of the cosmic radiation on living organisms in terrestrial conditions. Meanwhile, the global practice pattern of experiments with accelerators, as a rule, involves conducting acute exposures to the beams of monoenergetic charged particles of the same type. However, in space conditions, irradiation occurs over a long time in a low-intensity mixed radiation field both of electromagnetic (gamma rays) and corpuscular (neutrons and charged particles from protons up to nickel) nature with a highly wide energy range (from several MeV/nucleon to hundreds of GeV/nucleon), as it was shown by means of calculation previously [5]. From here it logically follows that the creation of the effects of irradiation of living organisms on accelerators and in real space flight conditions has different mechanisms, thus, a mixed radiation field can basically cause a synergistic effect [6]. Until recently, modeling of such a complex cosmic radiation in terrestrial conditions did not seem feasible. A particular interest in this problem has arisen in recent years with understanding of the role of heavy nuclei in inducing disorders of the central nervous system of astronauts.

Due to the specifics of cosmic radiation composed of GCR particles, radiobiological experiments with relativistic heavy nuclei can be conducted only on several accelerator facilities such as: the booster at the RHIC heavy-ion collider at Brookhaven National Laboratory (USA), where it is

feasible to obtain beams of nuclei up to uranium with an energy of up to 1.5 GeV/nucleon; the heavy-ion synchrotron at GSI (Germany) that provides nuclei up to uranium with an energy of up to 1 GeV/nucleon; the heavy-ion synchrotron Nuclotron at JINR (Russia), that, being part of the NICA complex, provides nuclei up to gold with an energy of up to 4.5 GeV/nucleon [7].

On these facilities several approaches to modeling of complex cosmic radiation fields have been proposed. The general principle is to use beams of the charged particle accelerators in order to form such a radiation field that is close either to the internal radiation field of the spacecraft or to the radiation field of primary GCR particles (ignoring shielding). For this purpose, a special unit, the so-called "GCR simulator", can be installed on the beam. The required radiation field is created behind the simulator, where biological objects for irradiation are placed.

NASA pioneered the creation of the GCR simulator. An "active" version of the GCR simulator has been developed on the basis of the booster at the RHIC heavy-ion collider in Brookhaven. That version is capable of sequentially delivering protons and HZE ions in order to simulate a mixed GCR field in the energy range up to 1 GeV/nucleon [8–10]. The quasi-continuous spectra of GCR particles are reproduced by means of a set of discretized monoenergetic beams of various nuclei that rapidly change during irradiation.

A fundamentally different approach to a simulator was suggested in the paper of Chancellor and his colleagues: only one beam of Fe ions with an energy of 1 GeV/nucleon and a complex polyethylene unit or a converter are applied [11]. This approach can be considered as "passive", which means that the beam parameters remain unchanged throughout the entire irradiation, and the necessary continuous energy spectra of all particles in the irradiation field are provided by a special converter, and, in doing so, irradiation is produced simultaneously by all types of particles.

Another GCR simulator was proposed by the European Space Agency [12]. The so-called "active-passive" or "hybrid" approach to modeling developed for the future FAIR facility at GSI can be considered as a further development of the two approaches mentioned above. In this case, a combination of geometrically complex beam modulators and a set of energies of Fe ions is used to create a necessary mixed radiation field. The main difference between this simulator and the previous (passive) one is the use of a set of three beam energies of Fe ions, in addition to beam modulators, therefore this approach can be considered as hybrid.

Researchers of the JINR Laboratory of Radiation Biology have proposed [13, 14] a new unique approach to modeling of a complex multicomponent internal radiation field of a spacecraft [5]. Hereinbelow, an analytical model of the proposed GCR simulator is described in detail, as well as the software being developed required for the implementation of the GCR simulator model: processing of the initial data obtained with Monte Carlo programs, fitting and optimization of model parameters as well as data visualization tools.

1. GENERAL DESCRIPTION OF THE GCR SIMULATOR MODEL

The proposed approach, as well as the version of the GCR simulator described by Chancellor and his colleagues [11], implies a use of a uniform beam of Fe ions with an energy of 1 GeV/nucleon; except that the beam irradiates special cylindrical converters with a diameter of 10 cm and a maximum length of up to 50 cm. Herein, the converters consist of sectoral segments (targets) of different lengths, as shown in Fig. 1. These converters can be made entirely of a single material, for example, polyethylene (homogeneous ones), or are composed of various materials, for example, polyethylene and iron (heterogeneous ones).

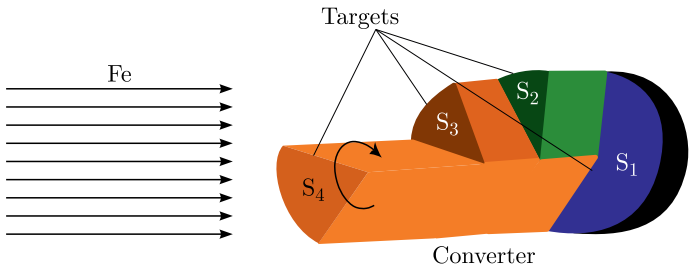

Fig. 1. A design diagram of a converter consisting of four targets for creation of a mixed radiation field at the irradiation site behind the GCR simulator. A wide beam of ^{56}Fe ions with an energy of 1 GeV/nucleon falls uniformly to the simulator

During the irradiation process, the converter rotates rapidly around the beam axis which makes it possible to achieve uniformity of the radiation field behind the simulator. With a uniformly incident field of the ^{56}Fe ions of the beam on a circular sector (target) with a fixed thickness, a uniform field of the required fragments is generated in the area behind this target. When the circular sector of the target rotates, the field with fragments fills the entire area of the converter circle. This is true for each sector forming a converter.

With a steady uniform beam of ^{56}Fe falling at the end of a rotating converter, the ratio of fluences of secondary particles from sectoral targets in the field behind the converter is proportional to the ratio of the areas of these sectors. The ratio of the target area with a certain thickness to the area of the entire surface of the converter end face is a mathematical weight for a given target in linear combination of the targets. A detailed description of all converter and simulator parameters is presented in Sec. 2.

Thus, provided the field of primary ^{56}Fe ions is uniform, the proposed design ensures uniformity of the fields of all secondary particles behind the simulator in the area of location of irradiated biological objects.

When creating a simulator, it is necessary to resolve a fundamental discrepancy between the charge distribution of fragments from the ^{56}Fe projectile and the charge distribution of cosmic radiation. The problem resides in the fact that when ^{56}Fe interacts with a target, peripheral collisions

are most likely to happen resulting in formation of predominantly nuclei of fragments with Z close to 26. On the contrary, protons and helium nuclei significantly predominate in the charge distribution of the radiation field inside the spacecraft [5]. For this reason, the simulator uses targets of different thicknesses, which are responsible for the formation of fragments with different Z groups, while their contribution to the overall charge distribution is regulated by appropriate weights (area of the sectors and exposure times).

In addition, it is extremely difficult to reproduce the spectra of all particles of the spacecraft's internal radiation field with only one converter since a set of a large number of target sectors is required the weights of many of which (especially those responsible for the formation of the heaviest fragments) will be extremely low compared to the targets themselves which generate mainly protons and α particles. So, it is reasonable to use not one but several interchangeable converters, which alternatively may have different exposure times. Therefore, the GCR simulator can be built in the form of a cylinder consisting of a certain number of converters (Fig. 2).

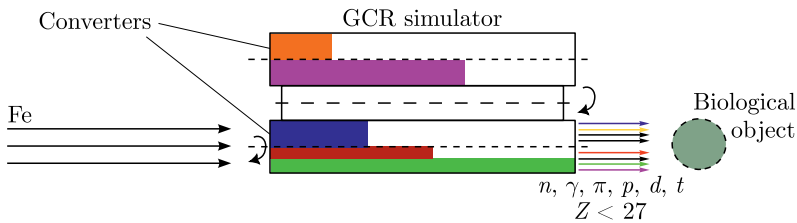

Fig. 2. The general scheme of the GCR simulator with several converters in the composition

Although the irradiation of converters occurs sequentially, they may interchange quickly (within several seconds), between accelerator pulses, which allows us to make suggestions about almost simultaneous exposure to all types of particles: neutrons, protons, $\pi^{\pm}$ mesons, γ quanta, light and heavy nuclei. Each converter recreates the energy spectra of a predominantly specific group of particles and is selected so that, during its rotation and irradiation, the required distributions over all types of particles of interest are recreated.

Hence, the proposed design of the GCR simulator has a number of advantages over the analogues. First, the proposed method makes it possible to reproduce all GCR nuclei with Z in the range from 1 to 27 with the required abundance. Secondly, the simulator reproduces continuous and broad energy spectra of the GCR particles (the maximum energy is being determined by the energy of the primary beam), which also determines a correct total fluence distribution over the linear energy transfer (LET) as well as partial contributions to the accumulated effective dose. Thirdly, rotation ensures uniformity of the fields of secondary particles behind the simulator. Fourthly, although the converters are being irradiated sequentially, each converter reproduces a mixed radiation field so the irradiation occurs simultaneously

with many different types of particles, which can be assimilated to the radiation conditions inside a spacecraft in space. Finally, the installation is relatively simple and can be implemented on accelerators capable of producing a uniform ^{56}Fe ion beam with an energy of 1 GeV/nucleon and does not imply additional adjustment of the entire accelerator system.

2. ANALYTICAL MODEL

2.1. Unit with a Single Converter. The converter hereafter refers to a cylinder composed of targets, a target being a cylindrical segment of a certain thickness, which may be made of one material (homogeneous one) or several (heterogeneous one). At its simplest, when the unit has only one converter ($K = 1$, where K is the total number of converters) and the whole exposure time spent on it, the fluence F_{Z,C_1} of a specified particle with atomic number Z after exposure of the C_1 converter (whole unit) is described as a linear combination as follows:

$$F_{Z,C_1} = A_{\text{tot}}^{-1} \sum_{i=1}^{N} a_{C_1,D_i} f_{Z,D_i} = \sum_{i=1}^{N} \frac{a_{C_1,D_i}}{A_{\text{tot}}} f_{Z,D_i} = \sum_{i=1}^{N} a'_{C_1,D_i} f_{Z,D_i}, \quad (1)$$

where A_{tot} is a total area of a converter end face, N is a total number of involved targets with various thicknesses, a_{C_1,D_i} is the area of the target sector with a thickness of D_i in the C_1 converter, f_{Z,D_i} is the fluence (normalized to one primary ion) of a particle with atomic number Z when irradiating a target with a thickness of D_i, obtained, for example, computationally using Monte Carlo-based FLUKA [15, 16] and PHITS [17] transport codes or by means of other programs.

To obtain the result fluence from the C_j converter (here $j = 1$), it is necessary to sum up the weighted contributions of fluences from the targets of different thicknesses included in it. The fluence contribution is different due to the different occupied area of the circular sectors, this contribution is taken into account by the normalized coefficients $a'_{C_1,D_i} = a_{C_1,D_i}/A_{\text{tot}}$, whereas $\sum\limits_{i=1}^{N} a_{C_1,D_i} = A_{\text{tot}}$.

Further, similarly to the case with a unit composed of a set of converters (see Subsec. 2.2, Eq. (5)), one only needs to put $P_{D_i} = a'_{C_1,D_i}$, that is, $F_Z = F_{Z,C_1}$.

2.2. Unit with Multiple Converters. In the general case, when the necessary radiation field cannot be provided by only one converter, the unit is made up of a certain number of them, moreover, each converter has a certain exposure time, which is set by additional coefficients. Similarly to Eq. (1), the fluence F_{Z,C_j} of the particle Z after irradiation of the C_j converter is as follows:

$$F_{Z,C_j} = A_{\text{tot}}^{-1} \sum_{i=1}^{N} a_{C_j,D_i} f_{Z,D_i} = \sum_{i=1}^{N} \frac{a_{C_j,D_i}}{A_{\text{tot}}} f_{Z,D_i} = \sum_{i=1}^{N} a'_{C_j,D_i} f_{Z,D_i}. \quad (2)$$

Since in this case we have $K > 1$ converters, the final fluence F_Z of the particle Z when irradiating the entire unit taking into account all coefficients is described as follows:

$$F_Z = T_{\text{tot}}^{-1} \sum_{j=1}^{K} t_{C_j} F_{Z,C_j} = \sum_{j=1}^{K} \frac{t_{C_j}}{T_{\text{tot}}} F_{Z,C_j} = \sum_{j=1}^{K} t'_{C_j} F_{Z,C_j}, \tag{3}$$

where T_{tot} is a total time of exposure of the entire unit, t_{C_j} — the time of exposure of the C_j converter.

All coefficients are normalized as follows:

$$\begin{gathered} \sum_{i=1}^{N} a_{C_j,D_i} = A_{\text{tot}}, \qquad \sum_{j=1}^{K} t_{C_j} = T_{\text{tot}}, \\ \sum_{i=1}^{N} \frac{a_{C_j,D_i}}{A_{\text{tot}}} = \sum_{i=1}^{N} a'_{C_j,D_i} = 1, \qquad \sum_{j=1}^{K} \frac{t_{C_j}}{T_{\text{tot}}} = \sum_{j=1}^{K} t'_{C_j} = 1. \end{gathered} \tag{4}$$

It is obvious that the a'_{C_j,D_i} coefficients responsible for the occupied area are equivalent to the t'_{C_j} coefficients, which are responsible for the exposure time. For example, if you reduce the area of the target but irradiate it for a longer time, the result will be similar. Therefore, as a matter of convenience, one combined coefficient will be used hereafter. Let us substitute Eq. (2) into Eq. (3) and combine the coefficients as follows:

$$\begin{aligned} F_Z &= \sum_{j=1}^{K} t'_{C_j} \left[\sum_{i=1}^{N} a'_{C_j,D_i} f_{Z,D_i} \right] = \\ &= \sum_{i=1}^{N} f_{Z,D_i} \sum_{j=1}^{K} t'_{C_j} a'_{C_j,D_i} = \\ &= \sum_{i=1}^{N} f_{Z,D_i} P_{D_i}, \end{aligned} \tag{5}$$

where

$$P_{D_i} = \sum_{j=1}^{K} t'_{C_j} a'_{C_j,D_i}. \tag{6}$$

For the case of a complex unit, this is a combined parameter since the contribution in terms of area is equivalent to the contribution in terms of exposure. For the case of a unit consisting of one converter when only one converter is irradiated all the time, $P_{D_i} = a'_{C_1,D_i}, T_{\text{tot}} = t'_{C_1} = 1$. In any case, normalization is performed as follows:

$$\sum_{i=1}^{N} P_{D_i} = 1. \tag{7}$$

The fluence F_Z of a particle Z is a fluence that is created behind the unit when it is irradiated taking into account all the coefficients. When the entire unit is being irradiated, all particles with $1 \leqslant Z \leqslant 26$ can be born, therefore we obtain a system of the following equations:

$$\begin{cases} \sum\limits_{i=1}^{N} f_{1,D_i} P_{D_i} = F_1, \\ \sum\limits_{i=1}^{N} f_{2,D_i} P_{D_i} = F_2, \\ \qquad\qquad \vdots \\ \sum\limits_{i=1}^{N} f_{26,D_i} P_{D_i} = F_{26}. \end{cases}$$

This system of equations determines the value of the fluence of all particles $1 \leqslant Z \leqslant 26$ behind the GCR simulator when it is irradiated with a uniform beam of ^{56}Fe ions. It should be noted that this approach is more universal, and primary particles may, in principle, be heavier. In this case, secondary particles will have a higher Z value.

Now let us assume that we have some reference values of particle fluences that need to be obtained using the GCR simulator. Reference values hereafter refer to those values that need to be obtained behind a unit during irradiation. These can be either particle fluences obtained directly from the primary GCR models, for example, as in [18, 19], or fluences of the spacecraft's internal radiation field calculated under certain conditions, for example, with different solar activity, as was done in [5, 20]. Then, taking $F_{Z,\text{ref}}$ as the fluence of the particle Z which needs to be recreated behind the unit, to ensure that the simulator correctly reproduces the radiation field for all the particles, it is necessary to obtain the parameters P_{D_i} so that

$$\begin{cases} \sum\limits_{i=1}^{N} f_{1,D_i} P_{D_i} = F_{1,\text{ref}}, \\ \sum\limits_{i=1}^{N} f_{2,D_i} P_{D_i} = F_{2,\text{ref}}, \\ \qquad\qquad \vdots \\ \sum\limits_{i=1}^{N} f_{26,D_i} P_{D_i} = F_{26,\text{ref}}. \end{cases}$$

This is a system of linear algebraic equations (SLAE), expressed in matrix form

$$f\mathbf{P} = \mathbf{F}, \tag{8}$$

where

$$f = \begin{pmatrix} f_{1,D_1} & f_{1,D_2} & \cdots & f_{1,D_N} \\ f_{2,D_1} & f_{2,D_2} & \cdots & f_{2,D_N} \\ \vdots & \vdots & \ddots & \vdots \\ f_{26,D_1} & f_{26,D_2} & \cdots & f_{26,D_N} \end{pmatrix}, \mathbf{P} = \begin{pmatrix} P_{D_1} \\ P_{D_2} \\ \vdots \\ P_{D_N} \end{pmatrix}, \mathbf{F} = \begin{pmatrix} F_{1,\text{ref}} \\ F_{2,\text{ref}} \\ \vdots \\ F_{26,\text{ref}} \end{pmatrix}.$$

Here, a restriction is imposed on the parameters that are physically responsible for the area and exposure time and, therefore, must be non-negative. It should also be taken into account that the results for the column vector $\mathbf{P}$ need to be normalized:

$$I = \sum_{i=1}^{N} P_{D_i}, \ \mathbf{P} = \begin{pmatrix} P_{D_1} \\ P_{D_2} \\ \vdots \\ P_{D_N} \end{pmatrix} I^{-1}.$$

The I number has a certain physical meaning that corresponds to the intensity (e. g., s^{-1}) of the hypothetical accelerator beam, at which the required radiation field is generated for the selected $F_{Z,\text{ref}}$ values. This is because all f_{Z,D_i} values are normalized to a single primary ^{56}Fe ion, and $F_{Z,\text{ref}}$ is the actual particle flux (e. g., $\text{cm}^{-2} \cdot \text{s}^{-1}$) to be achieved. Accordingly, in order to achieve the real fluence, it is necessary to multiply (5) by the intensity

$$F_{Z,\text{res}} = IF_Z. \tag{9}$$

In the above case, SLAE is set up for the fluences of all particles, which is an integral characteristic that does not take into account the specific energy distribution of particles. The spectra of fluences differential in energy (or LET) must also match the reference ones. Therefore, it is necessary to apply the same procedure for the distribution of fluences differential in energy and LET, where each equation is set up for a specific energy bin in the spectrum, based on a certain division of the continuous spectrum. Let us define $f_{\text{bin}}(E)$ as a matrix of bin values for the spectrum of the fluence differential in energy of any particle when irradiating the targets, and $\mathbf{F}_{\text{bin}}(E)$ as a vector of corresponding values in the reference spectrum. Similarly to Eq. (8), the matrix form is presented as

$$f_{\text{bin}}(E)\mathbf{P} = \mathbf{F}_{\text{bin}}(E). \tag{10}$$

The solution of system (10) is an approximation of a specific particle spectrum behind the GCR simulator to the reference spectrum at a given division. In order to take into account other spectra as well, it is necessary to supplement the equations with similar ones for all considered particles. Fluence spectra could be differentiated by LET, this will lead to similar equations:

$$f_{\text{bin}}(L)\mathbf{P} = \mathbf{F}_{\text{bin}}(L). \tag{11}$$

2.3. Selection and Optimization of Parameters. The problem of selecting the most appropriate coefficients can be solved using mathematical optimization, in this case, by minimization, using non-negative least squares (NNLS). This is because there is a constraint on the components of the $\mathbf{P}$ vector (they must be non-negative). The NNLS algorithm was proposed by Lawson and Hanson [21]. A variant of this algorithm is available in the SciPy module in Python as the `optimize.nnls` function, which uses the original Fortran code.

To apply this algorithm, it is necessary to rewrite Eq. (8) in a different way:

$$f_{\text{w}}\mathbf{P} = \mathbf{J}, \tag{12}$$

where

$$f_{\text{w}} = \begin{pmatrix} \frac{f_{1,D_1}}{F_{1,\text{ref}}} & \frac{f_{1,D_2}}{F_{1,\text{ref}}} & \dots & \frac{f_{1,D_N}}{F_{1,\text{ref}}} \\ \frac{f_{2,D_1}}{F_{2,\text{ref}}} & \frac{f_{2,D_2}}{F_{2,\text{ref}}} & \dots & \frac{f_{2,D_N}}{F_{2,\text{ref}}} \\ \vdots & \vdots & \ddots & \vdots \\ \frac{f_{26,D_1}}{F_{26,\text{ref}}} & \frac{f_{26,D_2}}{F_{26,\text{ref}}} & \dots & \frac{f_{26,D_N}}{F_{26,\text{ref}}} \end{pmatrix}, \mathbf{P} = \begin{pmatrix} P_{D_1} \\ P_{D_2} \\ \vdots \\ P_{D_N} \end{pmatrix}, \mathbf{J} = \begin{pmatrix} 1 \\ 1 \\ \vdots \\ 1 \end{pmatrix}.$$

This is done to remove the dependence on absolute values of fluences, and therefore f_{w} is weighted with the corresponding reference fluence values. This procedure can also be applied to Eqs. (10) and (11).

With due regard to the f_{w} (weighted) fluence matrix and the $\mathbf{J}$ all-ones vector, it is necessary to find such solutions that

$$\arg\min_{p} \|f_{\text{w}}\mathbf{P} - \mathbf{J}\|_2, \qquad p \geqslant 0. \tag{13}$$

Here, $p \geqslant 0$ means that each component of the $\mathbf{P}$ vector must be non-negative, and the problem reduces to finding such $\mathbf{P}$ coefficients, at which the Euclidean norm is minimal.

The parameters obtained by algorithm procedure are joint, they can be used for a unit with a single converter (see Subsec. 2.1), otherwise, if the sectors are very tiny, i. e., it will be technically problematic to fit them on one converter, the parameters can be split into a number of converters. If we want to get the $\mathbf{t}'$ coefficients from the found joint $\mathbf{P}$ coefficients, then the following simplest approach can be applied:

$$\begin{cases} a'_{C_1,D_1}t'_{C_1} + a'_{C_2,D_1}t'_{C_2} + \dots + a'_{C_K,D_1}t'_{C_K} = P_{D_1}, \\ a'_{C_1,D_2}t'_{C_1} + a'_{C_2,D_2}t'_{C_2} + \dots + a'_{C_K,D_2}t'_{C_K} = P_{D_2}, \\ \qquad\qquad\qquad\qquad\qquad\qquad\qquad\qquad \vdots \\ a'_{C_1,D_N}t'_{C_1} + a'_{C_2,D_N}t'_{C_2} + \dots + a'_{C_K,D_N}t'_{C_K} = P_{D_N}. \end{cases}$$

In matrix form,

$$a'\mathbf{t}' = \mathbf{P}, \tag{14}$$

where

$$a' = \begin{pmatrix} a'_{C_1,D_1} & a'_{C_2,D_1} & \cdots & a'_{C_K,D_1} \\ a'_{C_1,D_2} & a'_{C_2,D_2} & \cdots & a'_{C_K,D_2} \\ \vdots & \vdots & \ddots & \vdots \\ a'_{C_1,D_N} & a'_{C_2,D_N} & \cdots & a'_{C_K,D_N} \end{pmatrix}, \mathbf{t}' = \begin{pmatrix} t'_{C_1} \\ t'_{C_2} \\ \vdots \\ t'_{C_K} \end{pmatrix}, \mathbf{P} = \begin{pmatrix} P_{D_1} \\ P_{D_2} \\ \vdots \\ P_{D_N} \end{pmatrix}.$$

It comes to a SLAE similar to (8), which can be solved by the same approach, with known a' coefficients prescribed arbitrarily.

2.4. Model Quality Assessment. The R^2 metric (coefficient of determination) was chosen as a criterion for matching the results obtained from the simulator model, specified by some selected $\mathbf{P}$ coefficients to the reference values considered. The closer the R^2 value is to 1, the better the parameters allow us to approach the required reference spectra. To compare the models with each other, an adjusted R^2_{adj} coefficient of determination that can take negative values is used:

$$R^2_{\text{adj}} = 1 - \frac{\sum\limits_{i=1}^{n} \left(F_{i,\text{ref}} - \sum\limits_{j=1}^{N} f_{i,j} P_{D_j} \right)^2}{\sum\limits_{i=1}^{n} \left(F_{i,\text{ref}} - \frac{1}{n} \sum\limits_{i=1}^{n} F_{i,\text{ref}} \right)^2}. \tag{15}$$

A model is chosen with those parameters, the R^2 values of which are closest to 1 for all the considered spectra. It is important to note that this metric is only used to assess the quality of the data fit.

3. SOFTWARE IMPLEMENTATION OF THE GCR SIMULATOR MODEL

The implementation of the above model is provided by specially developed software. This software includes a full required feature set for processing data obtained from Monte Carlo particle transport codes, converting them to the format needed for compiling and solving of SLAE, optimizing parameters and determining quality of the model, and also includes tools for visualization, plotting and automatic generation of a report on the results obtained.

The software is written in the high-level programming language Python version 3.8 in an object-oriented paradigm. In fact, a software is a Python package, that is called `gcrs`. It contains a set of special modules with functions responsible for various aspects of modeling, as well as classes describing the characteristics of the simulator model.

The structure of the `gcrs` package code is presented in Fig. 3. To this date, the package consists of six modules, each of which contains a certain part of the functionality. The package includes a settings file in JSON format

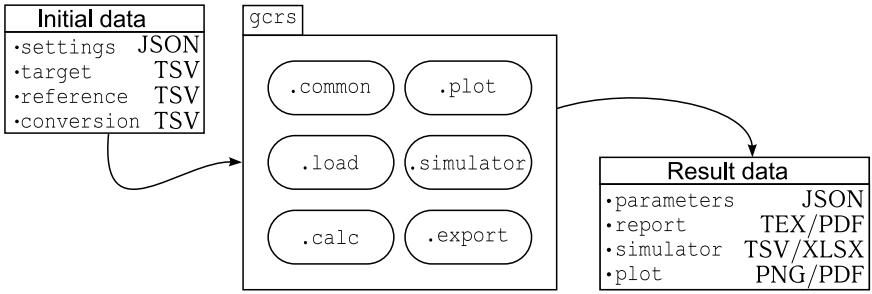

Fig. 3. Diagram of the source code structure of the software for the GCR simulator computer model

and source data in TSV format. New functionality is gradually being added to the package. The main current features of the software are described below.

The software uses energy spectra as source data as well as LET distributions of the flux of all particles formed behind targets of various thicknesses (`target` in Fig. 3) obtained using Monte Carlo transport codes. At the moment, the data obtained from FLUKA and PHITS are supported. This also includes reference data (`reference` in Fig. 3) which the simulator should recreate when it is irradiated. These data are also obtained from calculations using FLUKA or PHITS, support of other formats will be possibly added in future versions.

The `settings` file in JSON format contains all the settings needed for the correct operation of the software.

Conversion coefficients are used to calculate the absorbed and effective dose rate at the irradiation site behind the simulator (`conversion` in Fig. 3). To obtain conversion coefficients for determining the absorbed dose, data on ionization losses of particles from ATIMA code are used [22]. To determine the effective dose, data from the ICRP Publication 116 are used [23].

The module `common.py`, contains functions common to all modules of the `gcrs` package, responsible for working with paths, processing the settings file, etc. Here, third-party packages are also imported: `numpy`, `pandas`, `pylab`, `scipy`, `pylatex`.

The module `load.py`, responsible for uploading source data in formats specific to the Monte Carlo codes used, interprets them correctly and converts all data to a standard working format. The DataFrame class of the `pandas` package is used for all tabular data.

In the module `calc.py`, all the functions required for setting up a SLAE based on the initial data and its solution, as well as assessing the quality of the model, are defined. In addition, the functions necessary for determining doses at the irradiation site behind the simulator are also defined here.

The module `plot.py` provides plotting all source and result data, and `export.py` exports all the results obtained in TSV, XLSX, PNG, TEX, PDF, etc., formats. The module `export.py` contains the feature set necessary for

automatic generation of a report based on the results obtained in TEX and PDF formats, for which a third-party `pylatex` module is used.

In the module `simulator.py`, the classes required for a complete description of the simulator model are being implemented. Here, the main simulator class, which contains all the information on the simulator model and the parameters used, is defined.

4. RESULTS AND DISCUSSION

In order to demonstrate how the described approach and software work, let us define the simulator that recreates the inner radiation field of the spacecraft model on the basis of previous works [5, 13]. The detailed calculations were made for a simplified spacecraft model for the minimum and maximum solar activity (SA) cases, which can also be described via the values of the Wolf numbers: $W = 190$ for maximum SA and $W = 0$ for minimum SA. For the demonstration purposes, let us focus on the charge distribution of the secondary particles with Z ranging from 1 (protons) to 26 (iron nuclei). Similarly to Fig. 3 [13], Fig. 4 shows comparison between reference data and simulator model results.

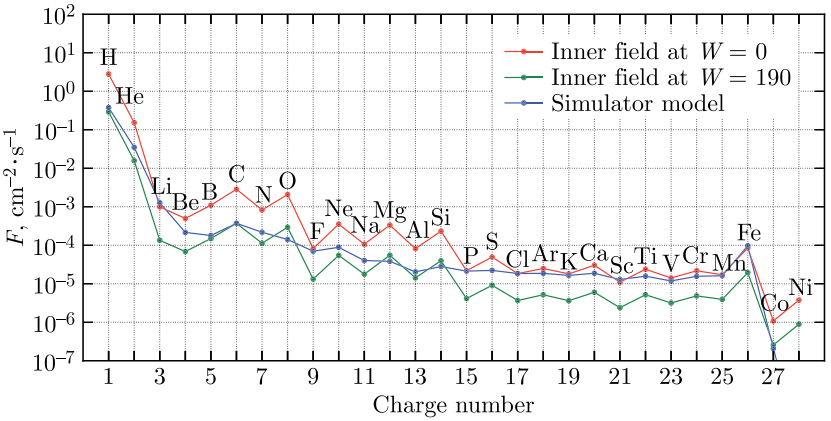

Fig. 4. Comparison of the charge distributions of the components of the radiation fields inside the spacecraft (taken as reference from [13]) at $W = 0$ (minimum SA) and $W = 190$ (maximum SA) with the charge distribution of secondary particles produced by the simulator model

To obtain the **P** vector for simulator description, `gcrs` needs precalculated values of f fluence matrix, which describes fluences of every particle considered at every chosen target type and thickness. These values for the f matrix, obtained from Monte Carlo codes, are stored in the default output format of those codes (which is specific to each code) as well as in TSV format. They are processed via the `gcrs` program in a specific way. For further calculations, we can use various precalculated sets of matrix values.

The reference **F** vector is also calculated using software based on the Monte Carlo codes data of the particle spectra by integrating over a specified energy range. In this case, the integrals were taken over the energy range from 10 to 1000 MeV/nucleon for the spectra at minimum SA ($W = 0$). These values can be defined arbitrarily, depending on the purpose of the simulation and the initial data used. Here, the maximum energy of the primary ^{56}Fe ions is 1 GeV/nucleon, so we are only considering parts of the spectra below this energy.

In the current example, the total number of equations for the SLAE is 546. The number of equations for the spectra with Z values between 1 and 26 is 520, as each spectrum has 20 energy bins. Additionally, there are 26 equations derived from integrals over the spectra in the form of Eq. (12). The number of targets used in the model is 13 (see Table 1), therefore the matrix f has dimensions 546×13. The solution to the SLAE using these targets is shown in Table 1.

Table 1. **Simulator model configuration based on the SLAE solution**

No.	Target type	Thickness D_i, cm	Weight P_{D_i}
1	Homogeneous $(CH_2)_n$	1	1.001E-04
2		8	3.604E-04
3		15	3.029E-04
4		17	2.169E-04
5		20	4.170E-04
6		23	2.446E-04
7		24	1.659E-04
8		25	1.206E-04
9		25.5	9.854E-05
10		26	2.760E-04
11		30	1.735E-03
12		50	7.241E-02
13	Heterogeneous $(CH_2)_n$ + Fe	30 + 20	9.236E-01

Based on the results of the solution, it is clear that these parameters need to be separated according to Eq. (14) in order to create a simulator with a few converters and avoid technical difficulties during production. This is what was done in the previous work [13]. The absolute reference values and simulator model results at the calculated intensity $I = 18.03$ ^{56}Fe ions per second are shown in Table 2. For each spectrum, the R^2 value is also provided, this metric is obtained over the energy range under consideration. The relative errors between the simulator results and the reference data are presented.

It can be seen that the charge distribution obtained with the simulator in general satisfactorily corresponds to the charge distribution of cosmic radiation in the considered SA range. These results are similar to those previously published in [13], where coefficients were found without

Table 2. **Optimization results for the simulator model**

Z	F, $cm^{-2} \cdot s^{-1}$			$\frac{\text{Simulator} - \text{SA}}{\text{SA}} \cdot 100$, %		R^2
	$W = 0$ (min SA)	$W = 190$ (max SA)	Simulator	$W = 0$ (min SA)	$W = 190$ (max SA)	
1	2.798E+00	2.908E-01	3.778E-01	–86.5	29.9	–0.832
2	1.525E-01	1.571E-02	3.499E-02	–77.1	122.7	–0.198
3	9.949E-04	1.346E-04	1.270E-03	27.7	844.1	0.287
4	4.962E-04	6.859E-05	2.158E-04	–56.5	214.6	0.244
5	1.096E-03	1.495E-04	1.793E-04	–83.6	19.9	–0.363
6	2.855E-03	3.708E-04	3.720E-04	–87.0	0.3	–0.481
7	8.251E-04	1.129E-04	2.178E-04	–73.6	92.8	–0.204
8	2.076E-03	2.926E-04	1.415E-04	–93.2	–51.6	–0.646
9	8.227E-05	1.321E-05	6.997E-05	–14.9	429.9	0.063
10	3.539E-04	5.466E-05	8.847E-05	–75.0	61.9	–0.307
11	1.067E-04	1.773E-05	4.012E-05	–62.4	126.3	–0.101
12	3.326E-04	5.498E-05	3.835E-05	–88.5	–30.2	–0.458
13	8.190E-05	1.425E-05	2.034E-05	–75.2	42.7	–0.073
14	2.321E-04	3.955E-05	2.803E-05	–87.9	–29.1	–0.369
15	2.184E-05	4.134E-06	2.130E-05	–2.5	415.1	0.637
16	4.946E-05	9.125E-06	2.224E-05	–55.0	143.7	0.324
17	1.845E-05	3.682E-06	1.847E-05	0.1	401.5	0.656
18	2.490E-05	5.179E-06	1.864E-05	–25.1	260.0	0.609
19	1.808E-05	3.633E-06	1.651E-05	–8.6	354.5	0.671
20	3.024E-05	6.020E-06	1.871E-05	–38.1	210.8	0.51
21	1.098E-05	2.392E-06	1.287E-05	17.3	438.2	0.537
22	2.381E-05	5.181E-06	1.574E-05	–33.9	203.8	0.555
23	1.413E-05	3.174E-06	1.184E-05	–16.2	272.9	0.601
24	2.171E-05	4.839E-06	1.562E-05	–28.1	222.8	0.578
25	1.711E-05	3.934E-06	1.619E-05	–5.4	311.5	0.584
26	8.533E-05	1.943E-05	9.687E-05	13.5	398.4	0.278

optimization algorithm being presented in the current work. This suggests that the proposed simulator is, indeed, a suitable solution for the given target and reference data. Although the relative error may seem significant at first glance, it is actually limited to the design of the simulator and the physical processes responsible for the formation of particles. These results suggest that the proposed simulator design could be used to reproduce the relative abundances of particles. In addition, the spectra of most secondary particles have a wide range of energies. Some of them fit well to the reference spectra, even if some do not match in absolute values. The biggest achievement, however, is the reproduction of particles with energies similar to those in the reference spectra. The largest difference is observed in regard to light nuclei and this limitation comes from physics, because the processes of nuclei

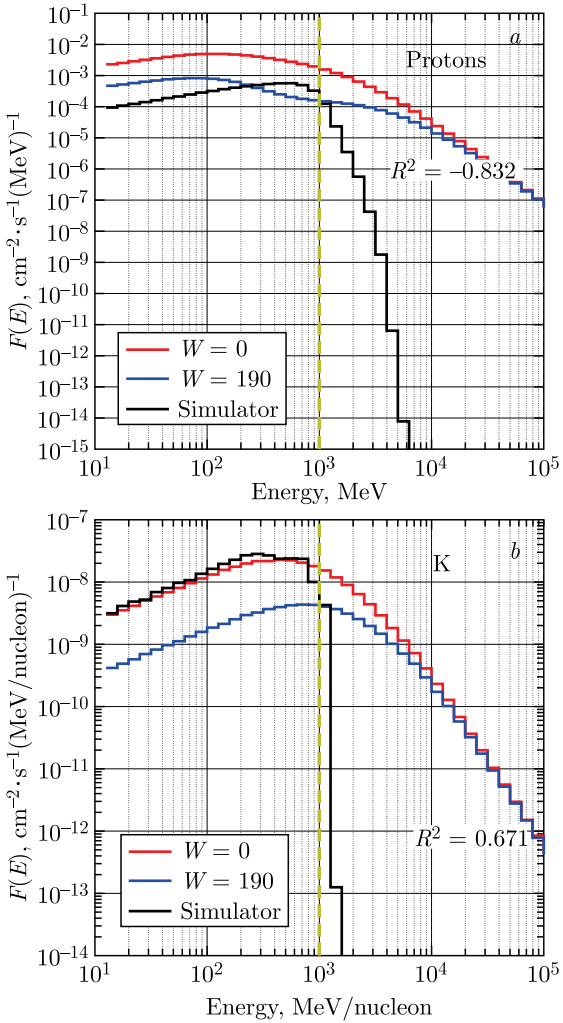

Fig. 5. Comparison of the proton (*a*) and potassium energy spectra (*b*) for the simulator model with the corresponding reference spectra (taken from [13]) at the minimum ($W = 0$) and maximum ($W = 190$) values of SA. The vertical yellow broken line indicates the upper limit of integral

formation in space and in the proposed approach are different in nature. In Fig. 5, the best and worst cases of spectra fitting are shown for protons and potassium ($Z = 19$) particles. The R^2 value was calculated for the range from 10 to 1000 MeV/nucleon. Although the proposed method does have some limitations, it has the potential to be improved and could become more effective with further development.

CONCLUSIONS

The paper presents a thorough review of the computer model of the GCR simulator originally proposed in [13]. A specially developed software designed for determining and configuring a computer model of a unit intended for irradiation with a mixed radiation field at charged particle accelerators is described. It should be noted that the program code is still under active development. The future plans include development of the `gcrs` package, with the aim of creating a universal tool that can determine and optimize simulator model parameters for other nuclei and energies and that will be able to import initial and reference data from other sources.

Acknowledgements. This work is inspired by the ideas of Professor G. N. Timoshenko who has passed away. We are deeply saddened by this loss and forever grateful for his significant contributions and for him being a truly good person.

The authors would like to express their gratitude to A. S. Gordeeva for her valuable assistance with the editorial process of the work.

Conflict of Interest. The authors declare that they have no known competing financial interests or personal relationships that could have appeared to influence the work reported in this paper.

REFERENCES

1. *Chancellor J. C., Scott G. B. I., Sutton J. P.* Space Radiation: The Number One Risk to Astronaut Health beyond Low Earth Orbit // Life. 2014. V. 4, No. 3. P. 491–510.
2. *Grigor'ev A. I., Krasavin E. A., Ostrovsky M. A.* The Problem of the Radiation Barrier during Piloted Interplanetary Flights // Her. Russ. Acad. Sci. 2017. V. 87, No. 1. P. 63–66; https://doi.org/10.1134/S1019331617010014.
3. Radiation in Space: Relevance and Risk for Human Missions / Eds. Ch. Hellweg, Th. Berger, D. Matthiä, Ch. Baumstark-Khan. Cham, Switzerland: Springer, 2020.
4. *Simpson J. A.* Elemental and Isotopic Composition of the Galactic Cosmic Rays // Annu. Rev. Nucl. Part. Sci. 1983. V. 33, No. 1. P. 323–382; https://doi.org/10.1146/annurev.ns.33.120183.001543.
5. *Timoshenko G. N., Gordeev I. S.* Simulation of Radiation Field inside Interplanetary Spacecraft // J. Astrophys. Astr. 2020. V. 41, No. 1. P. 5; https://doi.org/10.1007/s12036-020-9620-3.
6. *Ham D. W., Song B., Gao J., Yu J., Sachs R. K.* Synergy Theory in Radiobiology // Radiat. Res. 2018. V. 189. P. 225–237.
7. *Lednicky R.* Projects of Nuclotron Modernization and Nuclotron-Based Ion Collider Facility (NICA) at JINR // Phys. At. Nucl. 2008. V. 71, No. 9. P. 1514–1517; https://doi.org/10.1134/S1063778808090044.
8. *Kim M. H. Y., Rusek A., Cucinotta F. A.* Issues for Simulation of Galactic Cosmic Ray Exposures for Radiobiological Research at Ground-Based Accelerators // Front. Oncol. 2015. V. 5; https://www.frontiersin.org/articles/10.3389/fonc.2015.00122.

9. *Slaba T. C., Blattnig S. R., Norbury J. W., Rusek A., La Tessa C.* Reference Field Specification and Preliminary Beam Selection Strategy for Accelerator-Based GCR Simulation // Life Sci. Space Res. 2016. V. 8. P. 52–67; https://www.sciencedirect.com/science/article/pii/S2214552416000031.
10. *Simonsen L. C., Slaba T. C., Guida P., Rusek A.* NASA's First Ground-Based Galactic Cosmic Ray Simulator: Enabling a New Era in Space Radiobiology Research // PLoS Biol. 2020. V. 18, No. 5. P. e3000669; https://doi.org/10.1371/journal.pbio.3000669.
11. *Chancellor J. C., Guetersloh S. B., Blue R. S., Cengel K. A., Ford J. R., Katzgraber H. G.* Targeted Nuclear Spallation from Moderator Block Design for a Ground-Based Space Radiation Analog. arXiv:1706.02727. 2017.
12. *Schuy C., Weber U., Durante M.* Hybrid Active-Passive Space Radiation Simulation Concept for GSI and the Future FAIR Facility // Front. Phys. 2020. V. 8; https://www.frontiersin.org/articles/10.3389/fphy.2020.00337.
13. *Gordeev I. S., Timoshenko G. N.* A New Type of Ground-Based Simulator of Radiation Field inside a Spacecraft in Deep Space // Life Sci. Space Res. 2021. V. 30. P. 66–71; https://www.sciencedirect.com/science/article/pii/S2214552421000389.
14. *Timoshenko G. N., Gordeev I. S.* Reference Radiation Field for GCR Chronic Exposure Simulation // Phys. Part. Nucl. Lett. 2021. V. 18, No. 7. P. 799–805; https://doi.org/10.1134/S1547477121070128.
15. FLUKA: A Multi-Particle Transport Code / Eds. A. Ferrari, P. R. Sala, A. Fassò, J. Ranft. Geneva, Switzerland: CERN, 2005. 387 p.
16. *Ahdida C., Bozzato D., Calzolari D., Cerutti F., Charitonidis N., Cimmino A., Coronetti A., D'Alessandro G. L., Donadon Servelle A., Esposito L. S., Froeschl R., García Alía R., Gerbershagen A., Gilardoni S., Horváth D., Hugo G., Infantino A., Kouskoura V., Lechner A., Lefebvre B., Lerner G., Magistris M., Manousos A., Moryc G., Ogallar Ruiz F., Pozzi F., Prelipcean D., Roesler S., Rossi R., Sabaté Gilarte M., Salvat Pujol F., Schoofs P., Stránský V., Theis C., Tsinganis A., Versaci R., Vlachoudis V., Waets A., Widorski M.* New Capabilities of the FLUKA Multi-Purpose Code // Front. Phys. 2022. V. 9; https://www.frontiersin.org/article/10.3389/fphy.2021.788253.
17. *Sato T., Iwamoto Y., Hashimoto S., Ogawa T., Furuta T., Abe S. I., Kai T., Tsai P. E., Matsuda N., Iwase H., Shigyo N., Sihver L., Niita K.* Features of Particle and Heavy Ion Transport Code System (PHITS) Version 3.02 // J. Nucl. Sci. Technol. 2018. V. 55, No. 6. P. 684–690; https://doi.org/10.1080/00223131.2017.1419890.
18. *Matthiä D., Berger T., Mrigakshi A. I., Reitz G.* A Ready-to-Use Galactic Cosmic Ray Model // Adv. Space Res. 2013. V. 51, No. 3. P. 329–338; https://www.sciencedirect.com/science/article/pii/S0273117712005947.
19. *Slaba T. C., Whitman K.* The Badhwar–O'Neill 2020 GCR Model // Space Weather. 2020. V. 18, No. 6; https://doi.org/10.1029/2020SW002456.
20. *Timoshenko G. N., Gordeev I. S.* Computation of Linear Energy Transfer of Space Radiation in Biological Tissue Analog // Planet. Space Sci. 2021. V. 199; https://www.sciencedirect.com/science/article/pii/S0032063321000295.
21. *Lawson C. L., Hanson R. J.* Solving Least Squares Problems // J. Am. Stat. Assoc. 1997. V. 72, No. 360. P. 930–931; http://www.jstor.org/stable/2286501.

22. *Geissel H., Scheidenberger C., Malzacher P., Kunzendorf J., Weick H.* ATIMA. Darmstadt, Germany: GSI, 2021; https://web-docs.gsi.de/weick/atima/ (online; accessed: 2022-04-18).
23. *Petoussi-Henss N., Bolch W. E., Eckerman K. F., Endo A., Hertel N., Hunt J., Pelliccioni M., Schlattl H., Zankl M.* ICRP Publication 116. Conversion Coefficients for Radiological Protection Quantities for External Radiation Exposures // Ann. ICRP. 2010. V. 40. P. 1–257.

Received on April 2, 2024.

Редактор *В. В. Булатова*

Подписано в печать 30.05.2024.
Формат 60 × 90/16. Бумага офсетная. Печать цифровая.
Усл. печ. л. 1,50. Уч.-изд. л. 1,55. Тираж 105 экз. Заказ № 60882.

Издательский отдел Объединенного института ядерных исследований
141980, г. Дубна, Московская обл., ул. Жолио-Кюри, 6.
E-mail: publish@jinr.ru
www.jinr.ru/publish/